

# Omnidirectional Camera

DAVIDE SCARAMUZZA  
GRASP LAB  
UNIVERSITY OF PENNSYLVANIA

## Synonyms

- Panoramic camera, spherical camera, catadioptric camera, fisheye camera, wide-angle camera

## Related Concepts

- camera calibration
- pinhole camera
- radial distortion
- omnidirectional vision
- camera parameter (intrinsic, extrinsic)
- intrinsic parameter matrix
- structure from motion
- epipolar geometry

## Definition

An omnidirectional camera (from *omni*, meaning all) is a camera with a 360-degree field of view in the horizontal plane, or with a visual field that covers a hemisphere or (approximately) the entire sphere.

## Background

Most commercial cameras can be described as pinhole cameras, which are modeled by a perspective projection. However, there are projection systems whose geometry cannot be described using the conventional pinhole model because of the very high distortion introduced by the imaging device. Some of these systems are omnidirectional cameras.

There are several ways to build an omnidirectional camera. Dioptric cameras use a combination of shaped lenses (e.g., fisheye lenses; see figure 1a) and can reach a field of view even bigger than 180 degrees (i.e., slightly more than a hemisphere). Catadioptric cameras combine a standard camera with a shaped mirror — such as a parabolic, hyperbolic, or elliptical mirror — and provide 360-degree field of view in the horizontal plane and more than 100 degrees in elevation. In figure 1b you can see an example catadioptric camera using a hyperbolic mirror. Finally, polydioptric cameras use multiple cameras with overlapping field of view (figure 1c) and so far are the only cameras that provide a real omnidirectional (spherical) field of view (i.e.,  $4\pi$  steradians).

Catadioptric cameras were first introduced in robotics in 1990 by Yagi and Kawato [1], who used them for localizing robots. Fisheye cameras started to

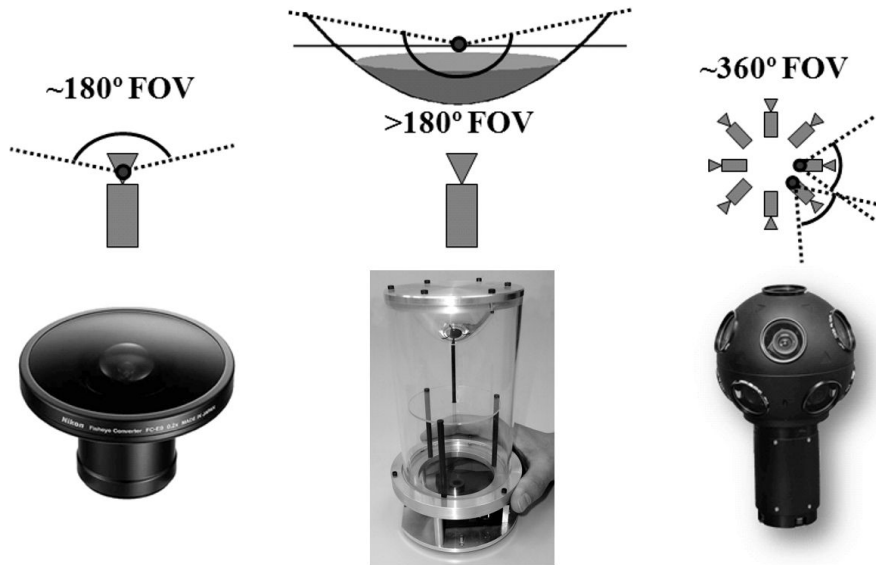


**Fig. 1.** (a) Dioptric camera (e.g. fisheye); (b) catadioptric camera; (c) an example polydioptric camera produced by Immersive Media.

spread over only in 2000 thanks to new manufacturing techniques and precision tools that led to an increase of their field of view up to 180 degrees and more. However, it is only since 2005 that these cameras have been miniaturized to the size of 1-2 centimeters, and their field of view has been increased up to 190 degrees or even more (see, for instance, figure 6a).

In the next sections, an overview on omnidirectional camera models and calibration will be given. For an in-depth study on omnidirectional vision, the reader is referred to [2,3,4], and to [5] for a more detailed survey on omnidirectional camera models.

## Theory

### 0.1 Central omnidirectional cameras

A vision system is said to be central when the optical rays to the viewed objects intersect in a single point in 3D called projection center or single effective viewpoint (figure 2). This property is called single effective viewpoint property. The perspective camera is an example of a central projection system because all optical rays intersect in one point, that is, the camera optical center.

All modern fisheye cameras are central, and hence, they satisfy the single effective viewpoint property. Central catadioptric cameras conversely can be built only by opportunely choosing the mirror shape and the distance between the

camera and the mirror. As proven by Baker and Nayar [6], the family of mirrors that satisfy the single viewpoint property is the class of rotated (swept) conic sections, that is, hyperbolic, parabolic, and elliptical mirrors. In the case of hyperbolic and elliptical mirrors, the single view point property is achieved by ensuring that the camera center (i.e., the pinhole or the center of the lens) coincides with one of the foci of the hyperbola (ellipse) (figure 3). In the case of parabolic mirrors, an orthographic lens must be interposed between the camera and the mirror, this makes it possible that parallel rays reflected by the parabolic mirror converge to the camera center (figure 3).

The reason a single effective viewpoint is so desirable is that it allows the user to generate geometrically correct perspective images from the pictures captured by the omnidirectional camera (figure 4). This is possible because, under the single view point constraint, every pixel in the sensed image measures the irradiance of the light passing through the viewpoint in one particular direction. When the geometry of the omnidirectional camera is known, that is, when the camera is calibrated, one can precompute this direction for each pixel. Therefore, the irradiance value measured by each pixel can be mapped onto a plane at any distance from the viewpoint to form a planar perspective image. Additionally, the image can be mapped on to a sphere centered on the single viewpoint, that is, spherical projection (figure 4, bottom).

Another reason why the single view point property is so important is that it allows the user to apply the well known theory of epipolar geometry, which is extremely important for structure from motion. Epipolar geometry holds for any central camera, both perspective and omnidirectional.

## 0.2 Omnidirectional camera model and calibration

Intuitively, the model of an omnidirectional camera is a little more complicated than a standard perspective camera. The model should indeed take into account the reflection operated by the mirror in the case of a catadioptric camera or the refraction caused by the lens in the case of a fisheye camera. Because the literature in this field is quite large, this chapter reviews two different projection models that have become standards in omnidirectional vision and robotics. Additionally, Matlab toolboxes have been developed for these two models, which are used worldwide by both specialists and non-experts.

The first model is known as the unified projection model for central catadioptric cameras. It was developed in 2000 by Geyer and Daniilidis [7] (later refined by Barreto and Araujo [8]), who have the merit of having proposed a model that encompasses all three types of central catadioptric cameras, that is, cameras using a hyperbolic, parabolic, or elliptical mirror. This model was developed specifically for central catadioptric cameras and is not valid for fisheye cameras. The approximation of a fisheye lens model by a catadioptric one is usually possible — however, with limited accuracy only — as investigated in [9].

Conversely, the second model unifies both central catadioptric cameras and fisheye cameras under a general model also known as Taylor model. It was developed in 2006 by Scaramuzza et al. [10,11] and has the advantage that both

catadioptric and dioptric cameras can be described through the same model, namely a Taylor polynomial.

### 0.3 Unified model for central catadioptric cameras

With their landmark paper from 2000, Geyer and Daniilidis showed that every catadioptric (parabolic, hyperbolic, elliptical) and standard perspective projection is equivalent to a projective mapping from a sphere, centered in the single viewpoint, to a plane with the projection center on the perpendicular to the plane and distant  $\epsilon$  from the center of the sphere. This is summarized in figure 5.

The goal of this section is to find the relation between the viewing direction to the scene point and the pixel coordinates of its corresponding image point. The projection model of Geyer and Daniilidis follows a four-step process. Let  $P = (x, y, z)$  be a scene point in the mirror reference frame centered in  $C$  (figure 5). For convenience, we assume that the axis of symmetry of the mirror is perfectly aligned with the optical axis of the camera. We also assume that the  $x$  and  $y$  axes of the camera and mirror are aligned. Therefore, the camera and mirror reference frames differ only by a translation along  $z$ .

- 1. The first step consists in projecting the scene point onto the unit sphere; therefore:

$$P_s = \frac{P}{\|P\|} = (x_s, y_s, z_s). \quad (1)$$

- The point coordinates are then changed to a new reference frame centered in  $C_\epsilon = (0, 0, -\epsilon)$ ; therefore:

$$P_\epsilon = (x_s, y_s, z_s + \epsilon). \quad (2)$$

Observe that  $\epsilon$  ranges between 0 (planar mirror) and 1 (parabolic mirror). The correct value of  $\epsilon$  can be obtained knowing the distance  $d$  between the foci of the conic and the latus rectum  $l$  as summarized in table 1. The latus rectum of a conic section is the chord through a focus parallel to the conic section directrix.

- $P_\epsilon$  is then projected onto the normalized image plane distant 1 from  $C_\epsilon$ ; therefore,

$$\tilde{m} = (x_m, y_m, 1) = \left( \frac{x_s}{z_s + \epsilon}, \frac{y_s}{z_s + \epsilon}, 1 \right) = g^{-1}(P_s). \quad (3)$$

- Finally, the point  $\tilde{m}$  is mapped to the camera image point  $\tilde{p} = (u, v, 1)$  through the intrinsic-parameter matrix  $K$ ; therefore,

$$\tilde{p} = K\tilde{m}, \quad (4)$$

where  $K$  is

$$K = \begin{bmatrix} \alpha_u & \alpha_u \cot(\theta) & u_0 \\ 0 & \alpha_v & v_0 \\ 0 & 0 & 1 \end{bmatrix} \quad (5)$$

- It is easy to show that function  $g^{-1}$  is bijective and that its inverse  $g$  is given by:

$$P_s = g(m) \propto \begin{bmatrix} x_m \\ y_m \\ 1 - \epsilon \frac{x_m^2 + y_m^2 + 1}{\epsilon + \sqrt{1 + (1 - \epsilon^2)(x_m^2 + y_m^2)}} \end{bmatrix}, \quad (6)$$

where  $\propto$  indicates that  $g$  is proportional to the quantity on the right-hand side. To obtain the normalization factor, it is sufficient to normalize  $g(m)$  onto the unit sphere.

Equation (6) can be obtained by inverting (3) and imposing the constraint that  $P_s$  must lie on the unit sphere and, thus,  $x_s^2 + y_s^2 + z_s^2 = 1$ . From this constraint we then get an expression for  $z_s$  as a function of  $\epsilon$ ,  $x_m$ , and  $y_m$ . More details can be found in [12].

**Table 1.**  $\epsilon$  values for different types of mirrors

| Mirror type | $\epsilon$                    |
|-------------|-------------------------------|
| Parabola    | 1                             |
| Hyperbola   | $\frac{d}{\sqrt{d^2 + 4l^2}}$ |
| Ellipse     | $\frac{d}{\sqrt{d^2 + 4l^2}}$ |
| Perspective | 0                             |

Observe that equation (6) is the core of the projection model of central catadioptric cameras. It expresses the relation between the point  $m$  on the normalized image plane and the unit vector  $P_s$  in the mirror reference frame. Note that in the case of planar mirror, we have  $\epsilon = 0$  and (6) becomes the projection equation of perspective cameras  $P_s \propto (x_m, y_m, 1)$ .

This model has proved to be able to describe accurately all central catadioptric cameras (parabolic, hyperbolic, and elliptical mirror) and standard perspective cameras. An extension of this model for fisheye lenses was proposed in 2004 by Ying and Hu [9]. However, the approximation of a fisheye camera through a catadioptric one works only with limited accuracy. This is mainly because, while the three types of central catadioptric cameras can be represented through an exact parametric function (parabola, hyperbola, ellipse), the projective models of fisheye lenses vary from camera to camera and depend on the lens field-of-view. To overcome this problem, a new unified model was proposed, which will be described in the next section.

#### 0.4 Unified model for catadioptric and fisheye cameras

This unified model was proposed by Scaramuzza et al. in 2006 [10,11]. The main difference with the previous model lies in the choice of the function  $g$ . To overcome the lack of knowledge of a parametric model for fisheye cameras, the

authors proposed the use of a Taylor polynomial, whose coefficients and degree are found through the calibration process. Accordingly, the relation between the normalized image point  $\tilde{m} = (x_m, y_m, 1)$  and the unit vector  $P_s$  in the fisheye (mirror) reference frame can be written as:

$$P_s = g(m) \propto \begin{bmatrix} x_m \\ y_m \\ a_0 + a_2\rho^2 + \dots + a_N\rho^N \end{bmatrix}, \quad (7)$$

where  $\rho = \sqrt{x_m^2 + y_m^2}$ . As the reader have probably noticed, the first-order term (i.e.,  $a_1\rho$ ) of the polynomial is missing. This follows from the observation that the first derivative of the polynomial calculated at  $\rho = 0$  must be null for both catadioptric and fisheye cameras (this is straightforward to verify for catadioptric cameras by differentiating (6)). Also observe that because of its polynomial nature, this expression can encompass catadioptric, fisheye, and perspective cameras. This can be done by opportunely choosing the degree of the polynomial. As highlighted by the authors, polynomials of order three or four are able to model very accurately all catadioptric cameras and many types of fisheye cameras available on the market. The applicability of this model to a wide range of commercial cameras is at the origin of its success.

## 0.5 Omnidirectional camera calibration

The calibration of omnidirectional cameras is similar to that for calibrating standard perspective cameras. Again, the most popular methods take advantage of planar grids that are shown by the user at different positions and orientations. For omnidirectional cameras, it is very important that the calibration images are taken all around the camera and not on a single side only. This in order to compensate for possible misalignments between the camera and mirror.

It is worth to mention three open-source calibration toolboxes currently available for Matlab, which differ mainly for the projection model adopted and the type of calibration pattern.

- The toolbox of Mei uses checkerboard-like images and takes advantage of the projection model of Geyer and Daniilidis discussed earlier. It is particularly suitable for catadioptric cameras using hyperbolic, parabolic, folded mirrors, and spherical mirrors. Mei’s toolbox can be downloaded from [13], while the theoretical details can be found in [14].
- The toolbox of Barreto uses line images instead of checkerboards. Like the previous toolbox, it also uses the projection model of Geyer and Daniilidis. It is particularly suitable for parabolic mirrors. The toolbox can be downloaded from [12], while the theoretical details can be found in [15] and [16].
- Finally, the toolbox of Scaramuzza uses checkerboard-like images. Contrary to the previous two, it takes advantage of the unified Taylor model for catadioptric and fisheye cameras developed by the same author. It works with catadioptric cameras using hyperbolic, parabolic, folded mirrors, spherical,

and elliptical mirrors. Additionally, it works with a wide range of fisheye lenses available on the market — such as Nikon, Sigma, Omnitech-Robotics, and many others — with field of view up to 195 degrees. The toolbox can be downloaded from [17], while the theoretical details can be found in [10] and [11]. Contrary to the previous two toolboxes, this toolbox features an automatic calibration process. In fact, both the center of distortion and the calibration points are detected automatically without any user intervention. This toolbox became very popular and is currently used at several companies such as NASA, Philips, Bosch, Daimler, and XSens.

## Application

Thanks to the camera miniaturization, to the recent developments in optics manufacturing, and to the decreasing prices in the cameras market, catadioptric and dioptric omnidirectional cameras are being more and more used in different research fields. Miniature dioptric and catadioptric cameras are now used by the automobile industry in addition to sonars for improving safety, by providing to the driver an omnidirectional view of the surrounding environment. Miniature fisheye cameras are used in endoscopes for surgical operations or on board microaerial vehicles for pipeline inspection as well as rescue operations. Other examples involve meteorology for sky observation.

Roboticians have also been using omnidirectional cameras with very successful results on robot localization, mapping, and aerial and ground robot navigation [18,19,20,21,22,23]. Omnidirectional vision allows the robot to recognize places more easily than with standard perspective cameras [24]. Furthermore, landmarks can be tracked in all directions and over longer periods of time, making it possible to estimate motion and build maps of the environment with better accuracy than with standard cameras, see figure 6 for some of examples of miniature omnidirectional cameras used on state-of-the-art micro aerial vehicles. Several companies, like Google, are using omnidirectional cameras to build photorealistic street views and three-dimensional reconstructions of cities along with texture. Two example omnidirectional images are shown in figure 7.

## Recommended Readings

- [1] Yagi, Y., Kawato, S. (1990). Panorama scene analysis with conic projection. IEEE International Conference on Intelligent Robots and Systems, Workshop on Towards a New Frontier of Applications
- [2] Benosman, R., Kang, S. (2001). Panoramic Vision: Sensors, Theory, and Applications. New York, Springer-Verlag
- [3] Daniilidis, K., Klette, R. (2006). Imaging Beyond the Pinhole Camera. New York, Springer
- [4] Scaramuzza, D. (2008). Omnidirectional vision: from calibration to robot motion estimation, PhD thesis n. 17635. PhD thesis, ETH Zurich
- [5] Sturm, P., Ramalingam, S., Tardif, J., Gasparini, S., Barreto, J. (2010). Camera models and fundamental concepts used in geometric computer vision. Foundations and Trends in Computer Graphics and Vision **6**(1–2)

- [6] (Baker, S., Nayar, S.). A theory of single-viewpoint catadioptric image formation. *International Journal of Computer Vision* **35**(2)
- [7] Geyer, C., Daniilidis, K. (2000). A unifying theory for central panoramic systems and practical applications. *European Conference on Computer Vision*
- [8] (Barreto, J.P., Araujo, H.). Issues on the geometry of central catadioptric image formation
- [9] Ying, X., Hu, Z. (2004). Can we consider central catadioptric cameras and fisheye cameras within a unified imaging model? *European Conference on Computer Vision, Lecture Notes in Computer Science, Springer Verlag*
- [10] Scaramuzza, D., Martinelli, A., Siegwart, R. (2006). A flexible technique for accurate omnidirectional camera calibration and structure from motion. *IEEE International Conference on Computer Vision Systems*
- [11] Scaramuzza, D., Martinelli, A., Siegwart, R. (2006). A toolbox for easy calibrating omnidirectional cameras. *IEEE International Conference on Intelligent Robots and Systems*
- [12] (Barreto, J.). Omnidirectional camera calibration toolbox for matlab (ocamcalib toolbox) <http://www.isr.uc.pt/~jpbar/CatPack/pag1.htm>.
- [13] (Mei, C.). Omnidirectional camera calibration toolbox for matlab <http://homepages.laas.fr/~cmei/index.php/Toolbox>.
- [14] Mei, C., Rives, P. (2007). Single view point omnidirectional camera calibration from planar grids. *IEEE International Conference on Robotics and Automation*
- [15] Barreto, J., Araujo, H. (2005). Geometric properties of central catadioptric line images and their application in calibration. *IEEE Transactions on Pattern Analysis and Machine Intelligence* **27**(8) 1237–1333
- [16] Barreto, J., Araujo, H. (2006). Fitting conics to paracatadioptric projection of lines. *Computer Vision and Image Understanding* **101**(3) 151–165
- [17] (Scaramuzza, D.). Omnidirectional camera calibration toolbox for matlab (ocamcalib toolbox) Google for "ocamcalib" or visit [http://robotics.ethz.ch/~scaramuzza/Davide\\_Scaramuzza\\_files/Research/OcamCalib\\_Tutorial](http://robotics.ethz.ch/~scaramuzza/Davide_Scaramuzza_files/Research/OcamCalib_Tutorial)
- [18] (Blosch, M., Weiss, S., Scaramuzza, D., Siegwart, R.). Vision based map navigation in unknown and unstructured environments. *IEEE International Conference on Robotics and Automation*
- [19] Bosse, M., Rikoski, R., Leonard, J., Teller, S. (2002). Vanishing points and 3d lines from omnidirectional video. *International Conference on Image Processing*
- [20] Corke, P., Strelow, D., Singh, S. (2004). Omnidirectional visual odometry for a planetary rover. *IEEE/RSJ International Conference on Intelligent Robots and Systems*
- [21] Scaramuzza, D., Siegwart, R. (2008). Appearance-guided monocular omnidirectional visual odometry for outdoor ground vehicles. *IEEE Transactions on Robotics, Special Issue on Visual SLAM* **24**(5)
- [22] Scaramuzza, D., Fraundorfer, F., , Siegwart, R. (2009). Real-time monocular visual odometry for on-road vehicles with 1-point ransac. *IEEE International Conference on Robotics and Automation*



- [23] Tardif, J., Pavlidis, Y., Daniilidis, K. (2008). Monocular visual odometry in urban environments using an omnidirectional camera. IEEE/RSJ International Conference on Intelligent Robots and Systems
- [24] Scaramuzza, D., Fraundorfer, F., Pollefeys, M. (2010). Closing the loop in appearance-guided omnidirectional visual odometry by using vocabulary trees. Robotics and Autonomous System Journal, Elsevier **58**(6)

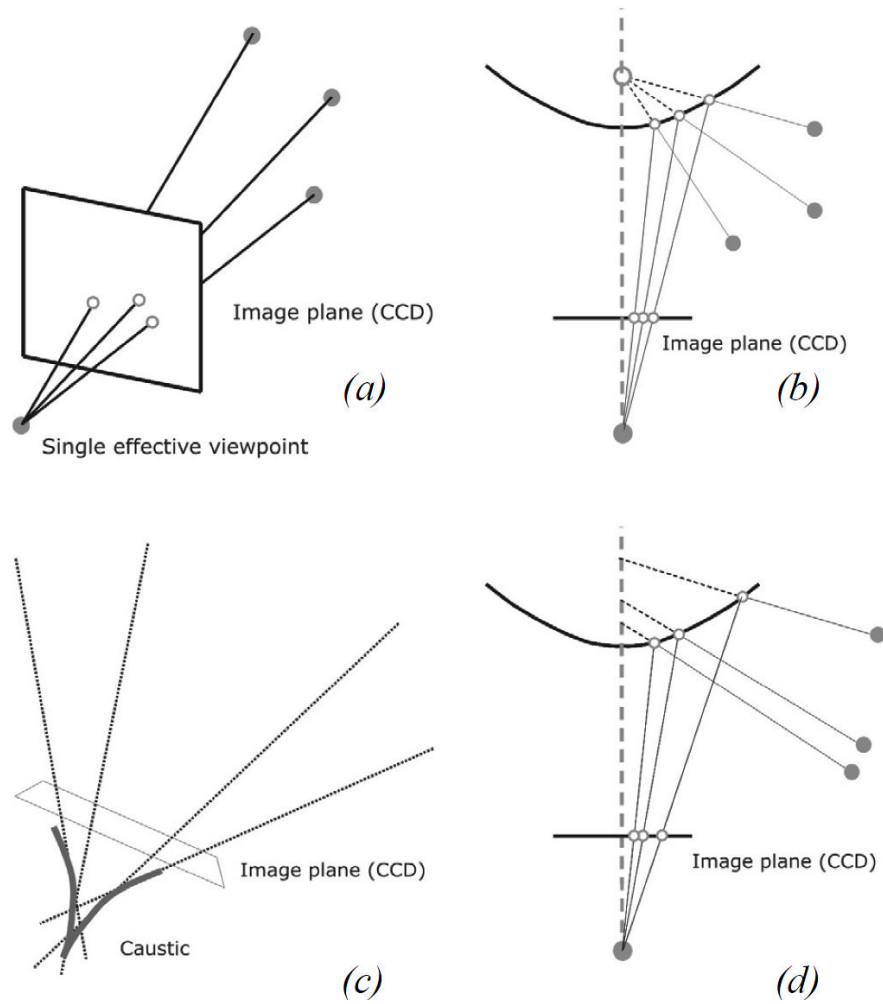


**Fig. 2.** (ab) Example of central cameras: perspective projection and catadioptric projection through a hyperbolic mirror. (cd) Example of noncentral cameras: the envelope of the optical rays forms a caustic.

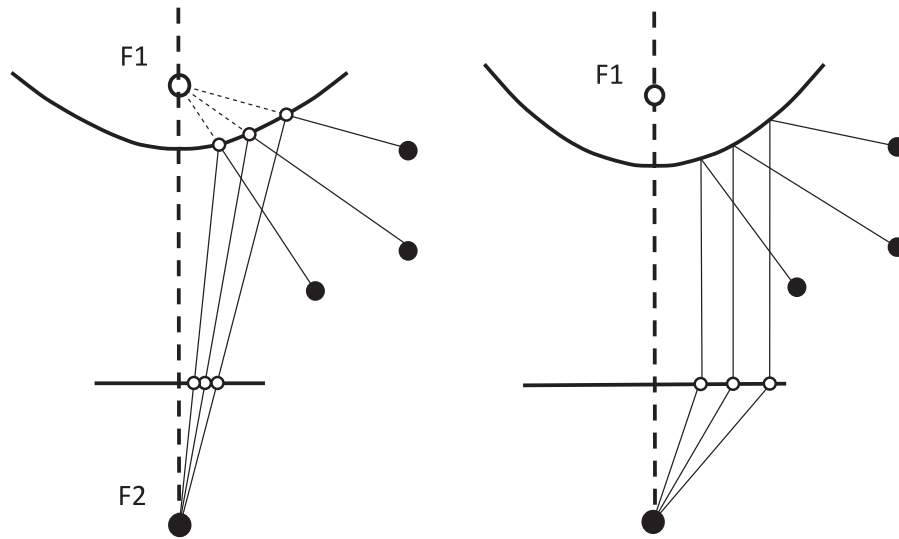


**Fig. 3.** Central catadioptric cameras can be built by using hyperbolic and parabolic mirrors. The parabolic mirror requires the use of an orthographic lens.

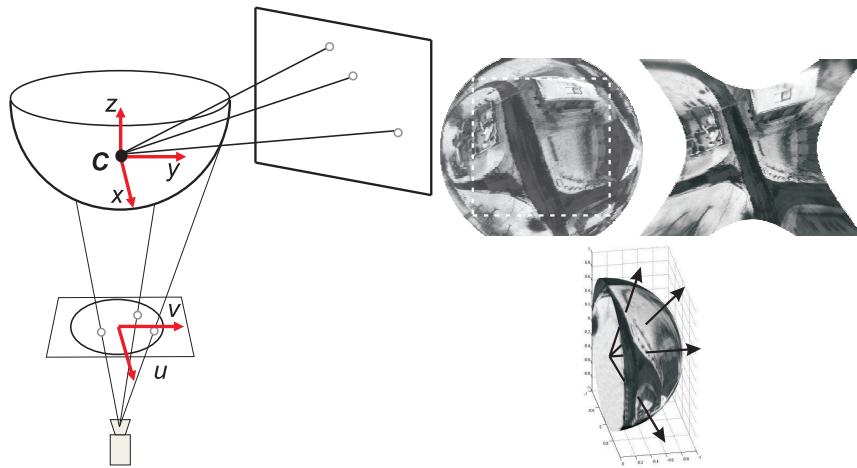


**Fig. 4.** Central cameras allow the user to remap regions of the omnidirectional image into a perspective image. This can be done straightforwardly by intersecting the optical rays with a plane specified arbitrarily by the user (a). For obvious reasons, we cannot project the whole omnidirectional image onto a plane but only subregions of it (b). Another alternative is the projection onto a sphere (c). In this case, the entire omnidirectional image can be remapped to a sphere.

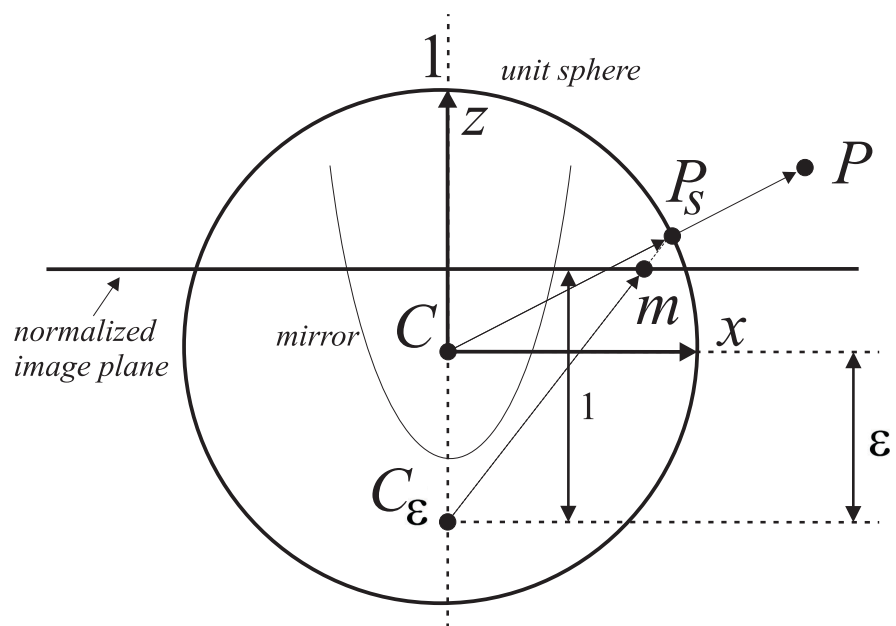


**Fig. 5.** Unified projection model for central catadioptric cameras of Geyer and Daniilidis.

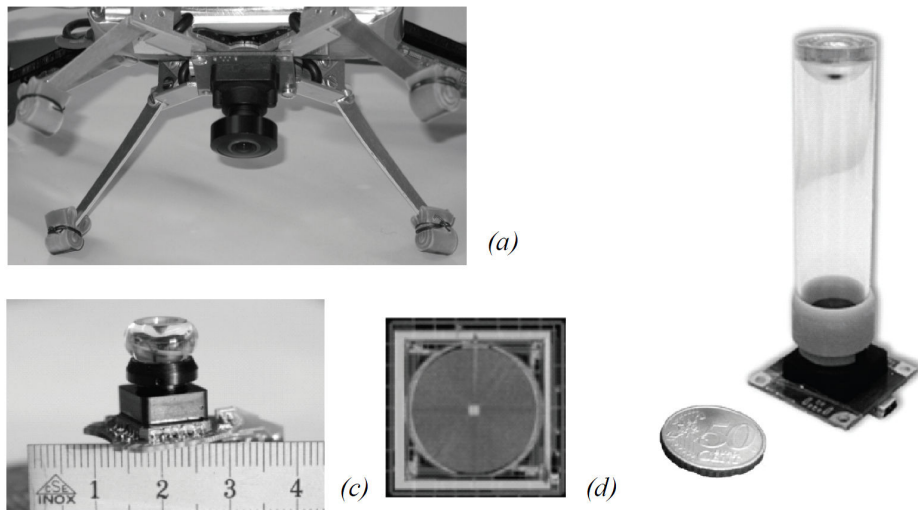
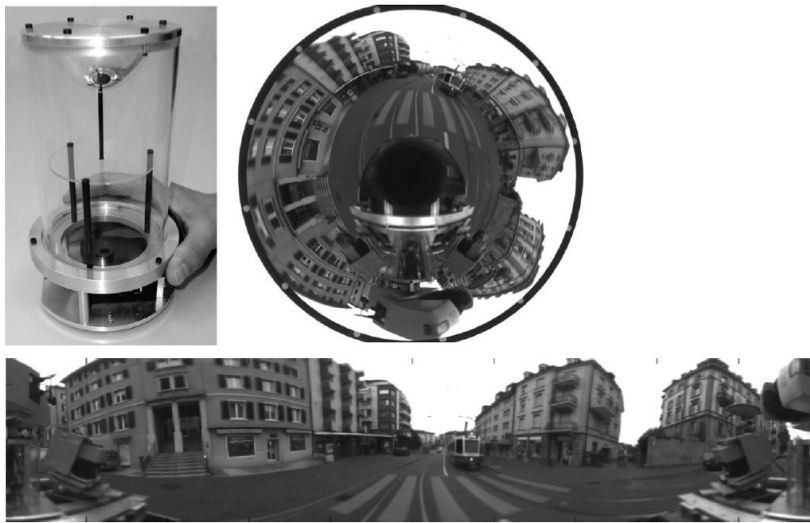
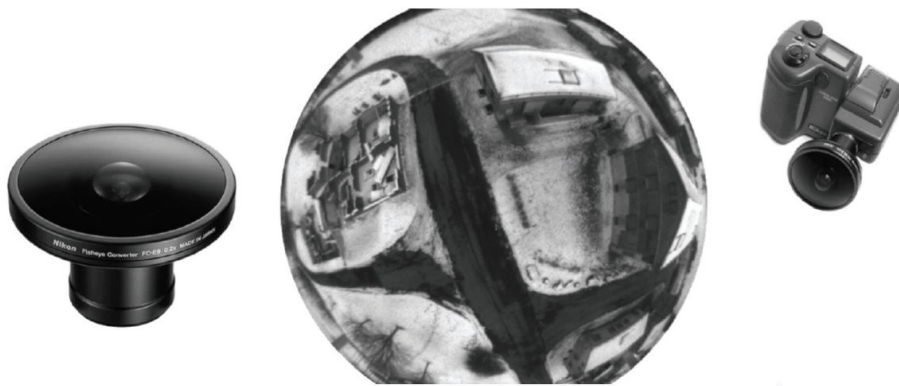


**Fig. 6.** (a) The fisheye lens from Omnitech Robotics ([www.omnitech.com](http://www.omnitech.com)) provides a field of view of 190 degrees. This lens has a diameter of 1.7 cm. This camera has been used on the sFly autonomous helicopter at the ETH Zurich, (section 2.4.3) [18]. (b) A miniature catadioptric camera built at the ETH Zurich, which is also used for autonomous flight. It uses a spherical mirror and a transparent plastic support. The camera measures 2 cm in diameter and 8 cm in height. (c) The muFly camera built by CSEM, which is used on the muFly helicopter at the ETH Zurich (section 2.4.3). This is one of the smallest catadioptric cameras ever built. Additionally, it uses a polar CCD (d) where pixels are arranged radially.



(a)



(b)

**Fig. 7.** (a) A catadioptric omnidirectional camera using a hyperbolic mirror. The image is typically unwrapped into a cylindrical panorama. The field of view is typically 100 degrees in elevation and 360 degrees in azimuth. (b) Nikon fisheye lens FC-E8. This lens provides a hemispherical (180 degrees) field of view.